Cross sections of discrete-level excitation of noble-gas atoms in Compton scattering

M. Ya. Amusia,[1,2] L. V. Chernysheva,[2] Z. Felfli,[3] and A. Z. Msezane[3]
[1]*Racah Institute of Physics, The Hebrew University, Jerusalem 91904, Israel*
[2]*A. F. Ioffe Physical-Technical Institute, St. Petersburg 194021, Russia*
[3]*Center for Theoretical Studies of Physical Systems, Clark Atlanta University, Atlanta, Georgia 30314*
(Received 11 February 2002; published 4 June 2002)

The differential cross section in angle and the total cross sections for the excitation of atomic discrete levels in Compton scattering are investigated. Results are presented for the valent $np-n,(n+1)d$ and $np-(n+1),(n+2)p$ levels of the outer subshells of the noble-gas atoms Ne, Ar, Kr, and Xe, covering the range of the momentum transferred to the atom up to 8 a.u., which is sufficiently large for the calculation of the total Compton excitation cross sections. Calculations were performed in one-electron Hartree-Fock approximation and with many-electron effects taken into account in the random-phase approximation with exchange for monopole, dipole, quadrupole, and octupole transitions. Contributions from higher multipoles proved to be unimportant and many-electron effects were found to be quite noticeable in the differential cross section, while almost negligible in the total excitation cross sections. We conclude that the contributions of discrete excitations are comparable to those of the ionization process.

DOI: 10.1103/PhysRevA.65.062705 PACS number(s): 34.80.Dp, 31.50.Df, 32.80.Dz, 34.10.+x

I. INTRODUCTION

In this paper we present results for the discrete-level excitation in the Compton scattering. We study this process in both the one-electron approximation and with account of many-electron correlations. The interest in Compton excitation is motivated to a large extent by the fact that in this process not only dipole, but also other multipole transitions may be investigated. The Compton scattering has also the advantage that its cross section is almost independent of the incoming photon frequency. This is in contrast to photoionization in which the cross section decreases very fast with the increase in photon energy ω. Compared to inelastic fast electron scattering where also nondipole excitations can be studied, the Compton scattering has two advantages. First, the effect of atomic core upon the incoming and outgoing electrons in their inelastic scattering is usually quite noticeable, at least at energies at which the cross section is measurable. This can modify the picture of electron excitation considerably, particularly for large momentum q transferred to the atom. In Compton scattering, the interaction of the incoming and outgoing photons with the core is negligible. Second, the fast electron inelastic scattering is dominated by the dipole transitions, while in Compton excitation these transitions are even suppressed when compared to the monopole and quadrupole ones. The largest drawback of Compton excitation studies is its small cross section.

For He, starting from $\omega=6$ keV the Compton scattering cross section $\sigma(\omega_i)$ becomes larger than the photoionization cross section $\sigma_\gamma(\omega_i)$ [1]. The same is true for the excitation process. For heavier atoms the corresponding lowest value of ω_i for which $\sigma(\omega_i)\geqslant\sigma_\gamma(\omega_i)$ increases rather fast with the growth of Z. Starting from some energy ω_i at which $\sigma(\omega_i)\geqslant\sigma_\gamma(\omega_i)$, it is the Compton ionization that determines the total-energy loss by a photon while interacting with an atom at $\omega\geqslant\omega_i$. Therefore, it is of interest to study the relationship between the Compton excitation and ionization cross sections of a given electron subshell of an atom in order to understand the relative role played by discrete excitation in the total atomic stopping power.

The main difference between Compton excitation and ionization, originates in the different role played by the electron binding to the nucleus. Without a nucleus atomic photoexcitation is impossible, since a free electron cannot absorb a photon. However, Compton scattering can proceed on a free electron [2]. The information about atomic structure obtained from the Compton process is different from the information obtained from both photoionization studies and fast electron inelastic scattering since the regions of space that play the most important roles in these processes are different. One should expect that the vicinity of the nucleus, which plays the key role in high-frequency photoionization, will not be emphasized in the Compton process. The inelastic electron-scattering cross section is determined by the period of time during which the incoming electron is reasonably close to the target atom. This period of time decreases with the growth of the incoming electron energy and so does the electron impact excitation cross section.

The generally small Compton excitation and ionization cross sections can be overcome only by the increase of the intensity of the incoming photon beam. Several sources of continuous spectrum of radiation now exist that generate very intense beams of high-frequency photons, up to $\omega=100$ keV. They were used recently [3,4] and, without doubt, will be used in the future to study Compton ionization and excitation. Also, it has been demonstrated recently that in order to obtain accurate enough calculated results even for the total accurately measured Compton ionization cross section [5,6], simple versions of the one-electron approximations are insufficient; the nonlocal nature of the one-electron potential has to be taken into account. This is why in this paper we use the Hartree-Fock nonlocal potential for the one-electron approximation.

Recently Compton one-electron and two-electron atomic ionization were investigated [7–13]. The main focus was on the He atom, but some analytical formulas valid for any atom

and ion were also obtained [8–10]. Expressions were derived and calculations performed for the ratio of double to single ionization cross sections [7,10,12] in He, particularly at high incoming photon energies. However, very little has been done about Compton excitation, particularly of atoms that are considerably more complicated than He and at relatively low energy transferred to the atom.

The aim of this paper is to fill in the gap by performing an investigation of Compton one-electron monopole, dipole, quadrupole, and octupole excitations of outer subshell electrons np^6 of Ne, Ar, Kr, and Xe. Thus, we have studied the region of relatively low energy transferred to the target atom ω, $\omega=\omega_{np-n,(n+1)d}^{L=1,3}$, $\omega=\omega_{np-(n+1);(n+2)s}^{L=1}$, and $\omega=\omega_{np-(n+1);(n+2)p}^{L=0,2}$ for momentum transferred q, $q\leqslant 8$ a.u. For this ω and in such a broad region of q-values multielectron correlations could be important. Therefore, we have performed calculations in the best one-electron Hartree-Fock (HF) approximation and with account of multielectron correlations in the random-phase approximation with exchange (RPAE). The RPAE has proved to be very effective in previous studies of atomic photoionization [14] and of inelastic scattering of fast electrons [15].

II. GENERAL EXPRESSIONS

The main features of this section are similar to those of our recent paper on Compton ionization [16]. However, for completeness we will repeat the main points of that paper. The operator that describes the interaction of photons with N atomic electrons in the nonrelativistic approximation is given by the expression

$$\vec{K}=\sum_{i=1}^{N}\left(-\frac{1}{c}\vec{p}_i\cdot\vec{A}(\vec{r}_i)+\frac{1}{2c^2}\vec{A}^2(\vec{r}_i)\right), \tag{1}$$

where $\vec{A}(\vec{r}_i)$ is the vector potential of the electromagnetic field, $\vec{r}_i$ and $\vec{p}_i$ are the ith electron's coordinate and momentum, respectively, while c is the speed of light (atomic units are used throughout this paper: $m_e=e=\hbar=1$, with m_e being the electron mass, e its charge and $\hbar$ the Planck constant). The cross section for inelastic or Compton scattering of a photon is expressed via the second power of $\vec{p}_i\cdot\vec{A}(\vec{r}_i)/c$ and the first power of $\vec{A}^2(\vec{r}_i)/2c^2$ operators. But the contribution of the $\vec{p}_i\cdot\vec{A}(\vec{r}_i)/c$ term to Compton scattering by nonrelativistic electrons is small.

For an external electromagnetic field one has $\vec{A}(\vec{r}_i)=\vec{\epsilon}\exp(i\vec{k}\cdot\vec{r})$. Therefore the differential cross section in scattering angle $d\Omega$ for Compton scattering accompanied by an atomic transition from the initial state $|i\rangle$ to the final state $|f\rangle$, $d\sigma_{if}(\omega)/d\Omega$ can be expressed via the matrix elements of the operator $\exp(i\vec{k}\cdot\vec{r})$ as

$$\frac{d\sigma_{if}(\omega_{fi})}{d\Omega}=\left(\frac{d\sigma}{d\Omega}\right)_{cl}\frac{E-\omega_{fi}}{E}\sum_f\left\langle i\left|\sum_{j=1}^{N}e^{i\vec{q}\cdot\vec{r}_j}\right|f\right\rangle^2. \tag{2}$$

Here E is the incoming photon energy and ω is the energy transferred to the atom in the scattering process, $(d\sigma/d\Omega)_{cl}$ is the classical Thompson scattering cross section of light from an electron (see [2]) and q is the momentum transferred to the atom in the process of Compton scattering, $\vec{q}=\vec{k}-\vec{k}'$ with $\vec{k}'$ being the outgoing photon momentum. The summation over final states f is performed preserving the energy conservation, $\omega_{fi}=E_f-E_i$, where E_f and E_i are the energies of the atom in the initial state and in the final state, respectively.

The squared term in Eq. (2) can be expressed via the generalized oscillator strengths (GOS's), which determine the inelastic scattering cross section of a fast charge particle upon an atom [17]

$$G_{fi}(\omega_{fi},q)=\frac{2\omega_{fi}}{q^2}\left|\sum_{j=1}^{N}\int\psi_f^*(\vec{r}_1,\ldots,\vec{r}_N)\exp(i\vec{q}\cdot\vec{r}_j)\psi_i(\vec{r}_1,\ldots,\vec{r}_N)d\vec{r}_j\right|^2$$
$$=\frac{2\omega_{fi}}{q^2}\left|\left\langle i\left|\sum_{j=1}^{N}e^{i\vec{q}\cdot\vec{r}_j}\right|f\right\rangle\right|^2. \tag{3}$$

Here $\psi_i(\vec{r}_1,\ldots,\vec{r}_N)$ and $\psi_f(\vec{r}_1,\ldots,\vec{r}_N)$ are the initial- and final-state atomic wave functions. With the help of Eq. (3), Eq. (2) can be presented as

$$\frac{d\sigma_{if}(\omega_{fi})}{d\Omega}=\left(\frac{d\sigma}{d\Omega}\right)_{\gamma}\frac{E-\omega_{fi}}{E}\frac{q^2}{2\omega_{fi}}\sum_f G_{fi}(\omega_{fi},q). \tag{4}$$

Compton scattering is of interest at high energies, so one has the limitation $\omega_{fi}/E\ll 1$. Neglecting terms of order $\omega_{fi}/E\ll 1$, one obtains the following relation:

$$q=\frac{2E}{c}\left(1-\frac{\omega_{fi}}{2E}\right)^{1/2}\sin\vartheta, \tag{5}$$

where $\vartheta=\theta/2$ and θ is the scattering angle of the outgoing photon. Thus, for a given value E the angle θ determines the momentum q and vice versa.

III. CROSS SECTIONS IN HF AND RPAE

In the Hartree-Fock approximation the Compton scattering cross section simplifies considerably, because the expres-

sion Eq. (3) that enters Eq. (4) reduces to

$$g_{st}(\omega_{fi},q)=\frac{2\omega_{fi}}{q^2}\left|\int \phi_s^*(\vec{r})\exp(i\vec{q}\cdot\vec{r})\phi_t(\vec{r})d\vec{r}\right|^2$$

$$=\frac{2\omega_{fi}}{q^2}|\langle s|\hat{B}(q)|t\rangle|^2. \quad (6)$$

Here $\phi_s(\vec{r})$ and $\phi_t(\vec{r})$ are HF wave functions of one-electron states with energies ϵ_f and ϵ_i, respectively, and $\hat{B}(q)=\exp(i\vec{q}\cdot\vec{r})$. The expression for the Compton scattering cross section in HF follows from Eq. (4) and is given by

$$\frac{d\sigma_{HF}(\omega_{fi})}{d\Omega}=\left(\frac{d\sigma}{d\Omega}\right)_{cl}\frac{E-\omega_{fi}}{E}\frac{q^2}{2\omega_{fi}}\sum_{s,t} g_{st}(\omega_{fi},q). \quad (7)$$

Here the summation is performed over all one-electron states with energies ϵ_f (for s) and ϵ_i (for t), which satisfy the energy-conservation restriction, $\epsilon_f=\omega_{fi}+\epsilon_i$.

The next step in our consideration of Compton scattering is to take into account many-electron correlations in the RPAE framework. This approximation has been applied very successfully to photoionization studies [14]. It gave quantitatively a good description of the cross sections, including a number of their specific features, such as giant resonances (GR) in the absolute cross sections and interference resonances (IR) in the partial ones. The RPAE is still very successful in describing new experimental data in this field, e.g., data on photon absorption by iodine [18], on nondipole corrections to the photoelectron angular distributions in noble gases [19] and on the generalized oscillator strengths for, e.g., Ar discrete excited levels [20] (the data [20] are described in [21]).

To obtain the Compton scattering cross section in RPAE, we replace $g_{st}(\omega_{fi},q)$ by $G^R_{st}(\omega_{fi},q)$. The latter is expressed via the matrix elements $\langle s|\hat{B}_R(\omega_{fi},q)|t\rangle$ of the Compton operator $\hat{B}_R(\omega_{fi},q)$ in the RPAE framework. In order to obtain $\hat{B}_R(\omega_{fi},q)$, an integral equation has to be solved. This equation can be presented symbolically as [16]

$$\hat{B}_R(\omega_{fi},q)=\hat{B}(q)+\hat{B}_R(\omega_{fi},q)\hat{\chi}(\omega_{fi})\hat{U}. \quad (8)$$

Here $\hat{\chi}(\omega)\equiv(\omega-\hat{H}_{ev})^{-1}-(\omega+\hat{H}_{ev})^{-1}$ describes the propagation of noninteracting virtually created electron and vacancy with the Hamiltonian $\hat{H}_{ev}$; $\hat{U}$ denotes the combination of direct and exchange terms of the interelectron Coulomb potential $V_{12}=1/|\vec{r}_1-\vec{r}_2|$. Equation (8) can be solved also symbolically leading to the following expression:

$$\hat{B}_R(\omega_{fi},q)=\frac{\hat{B}(q)}{[\hat{1}-\hat{\chi}(\omega_{fi})]\hat{U}}. \quad (9)$$

Nonsymbolically Eq. (8) is usually presented in a matrix form that looks more complicated than Eq. (8),

$$\langle s|\hat{B}_R(\omega_{fi},q)|t\rangle=\langle s|\exp(i\vec{q}\cdot\vec{r})|t\rangle$$
$$+\left(\sum_{n'\leqslant F,k'>F}-\sum_{n'>F,k'\leqslant F}\right)$$
$$\times\frac{\langle k'|\hat{B}_R(\omega,q)|n'\rangle\langle n's|U|k't\rangle}{\omega_{fi}-\epsilon_{k'}+\epsilon_{n'}+i\eta(1-2n_{k'})}. \quad (10)$$

Here, as in Eq. (7), $\leqslant F(>F)$ denotes occupied (vacant) HF states, ϵ_n are the one-electron HF energies, $\langle ns|U|kt\rangle=\langle ns|V|kt\rangle-\langle ns|V|tk\rangle$; while $\eta\to 0$ and $n_k=1(0)$ for $k\leqslant F(>F)$. The procedure of solving this equation is described in details [14,22]. Note that contrary to $\hat{B}(q)$, $\hat{B}_R(\omega,q)$ is a nonlocal operator, which corresponds to two space coordinates $\mathbf{r}$ and $\mathbf{r}'$ instead of only one, $\mathbf{r}$, in $\hat{B}(q)$.

IV. DETAILS OF CALCULATIONS

Discrete excitations are characterized by their energy, angular momentum, and spin. Using the Compton scattering operator considered above, only singlet states can be excited, but they can have different total momentum L. This is why one has to solve Eq. (10) separately for different multipoles. To do so, let us use the well-known expansion

$$\exp(i\vec{q}\cdot\vec{r})=\sum_{L=0}^{\infty}(2L+1)j_L(qr)P_L(\cos\zeta). \quad (11)$$

Here $j_L(qr)$ is the spherical Bessel function, $P_L(\cos\zeta)$ is the Legendre polynomial, and ζ is the angle between the vectors $\vec{q}$ and $\vec{r}$. Separating the angular parts of the one-electron HF wave functions, using Eq. (11) and performing analytically the integration over angles in the matrix elements in Eq. (6), instead of $g_{st}(\omega,q)$ partial one-electron GOS's $g^L_{nl,\epsilon l'}(\omega,q)$ can be introduced, with l' within the limits $|L-l|\leqslant l'\leqslant L+l$.

Equation (8) for $\hat{B}_R(\omega,q)$ with the help of Eq. (11) decouples into a system of independent equations for partial contributions, with given angular momentum L, $\hat{B}_{R^L}(\omega,q)$. These equations were solved numerically as is described in [22] giving matrix elements $\langle nl|\hat{B}_{R^L}(\omega_{fi},q)|\epsilon l'\rangle$. With these matrix elements the RPAE values can be obtained

$$G^{R(L)}_{nl,\epsilon l'}(\omega_{fi},q)=\frac{2\omega_{fi}}{q^2}|\langle nl|\hat{B}^{(L)}_R(\omega_{fi},q)|\epsilon l'\rangle|^2. \quad (12)$$

In numerical calculations we limit ourselves to monopole, dipole, quadrupole, and octupole, $L=0,1,2,3$ transitions. We calculate $g^L_{nl,n'l'}(\omega_{fi},q)$ and $G^{R(L)}_{nl,n'l'}(\omega_{fi},q)$ in a rather broad range of q values, $0\leqslant q\leqslant 8$ a.u. For values of E, $E>1000$ Ry, one can simplify Eq. (5), reducing it to

$q=(2E/c)\sin(\theta/2)$. For small scattering angles it reduces to $q=E\theta/c$. Then instead of Eq. (7) one obtains in HF approximation

$$\zeta^{HF}_{nl,n'l',L}(\omega_{fi},q)\equiv\frac{d\sigma^{HF}_{nl,n'l',L}(\omega_{fi})}{d\Omega}\Bigg/\left(\frac{d\sigma}{d\Omega}\right)_{cl}$$

$$=\frac{q^2}{2\omega_{fi}}g_{nl,n'l',L}(\omega_{fi},q) \tag{13}$$

$$q=(2E/c)\sin\theta/2,$$

and in RPAE

$$\zeta^{R}_{nl,n'l',L}(\tilde{\omega}_{fi},q)\equiv\frac{d\sigma^{R}_{nl,n'l',L}(\tilde{\omega}_{fi})}{d\Omega}\Bigg/\left(\frac{d\sigma}{d\Omega}\right)_{cl}$$

$$=\frac{q^2}{2\tilde{\omega}_{fi}}G^{R}_{nl,n'l',L}(\tilde{\omega}_{fi},q). \tag{14}$$

Here $\tilde{\omega}_{fi}$ is the RPAE value of the excitation energy considered, which in HF approximation is equal to ω_{fi}. The details and formulas that permit one to determine $\tilde{\omega}_{fi}$ can be found in [22].

The relative role of RPAE correlations in the excitation of an atom in Compton scattering is determined according to Eqs. (13) and (14) by the ratio

$$\eta_{nl,n'l',L}(\tilde{\omega}_{fi},\omega_{fi},q)=\frac{d\sigma^{R}_{nl,n'l',L}(\tilde{\omega}_{fi})}{d\Omega}\Bigg/\frac{d\sigma^{HF}_{nl,n'l',L}(\omega_{fi})}{d\Omega}$$

$$=G^{R}_{nl,n'l',L}(\tilde{\omega}_{fi},q)/g_{nl,n'l',L}(\omega_{fi},q). \tag{15}$$

If levels with the same $nl,n'l'$ but different values of L have the energies that cannot be separated in a given experiment, the effective value of $\xi^{HF,R}_{nl,n'l'}(\bar{\omega},q)$ is given by

$$\xi^{HF,R}_{nl,n'l'}(\bar{\omega},q)=\sum_L\ \zeta^{HF,R}_{nl,n'l',L}(\bar{\omega},q)$$

$$=\sum_L\ \frac{d\sigma^{HF,R}_{nl,n'l',L}(\bar{\omega})}{d\Omega}\Bigg/\left(\frac{d\sigma}{d\Omega}\right)_{cl}$$

$$=\sum_L\ \frac{q^2}{2\omega}G^{HF,R}_{nl,n'l',L}(\bar{\omega},q), \tag{16}$$

where $\bar{\omega}$ is the average excitation energy of the group of levels considered. The cross section for Compton excitation of the levels considered can be obtained by integrating Eq. (16) over $d\Omega$,

$$\sigma^{HF,R}_{nl,n'l'}(\bar{\omega})=2\pi\frac{c^2}{E^2}\int\left(\frac{d\sigma}{d\Omega}\right)_{cl}\xi^{HF,R}_{nl,n'l'}(\bar{\omega},q)q\,dq. \tag{17}$$

If several excitation levels are so close together in energy that they cannot be distinguished experimentally, the total differential Compton cross section for a given set of such levels in HF and RPAE can be obtained from Eqs. (14) and (15) by performing the summation over all the corresponding contributions,

$$\xi^{HF,R}_{nl}(\bar{\omega},q)=\sum_{n'l'\in\bar{\omega},L}\zeta^{HF,R}_{nl,n'l',L}(\bar{\omega},q)$$

$$=\sum_{n'l'\in\bar{\omega},L}\frac{d\sigma^{HF,R}_{nl,n'l',L}(\bar{\omega})}{d\Omega}\Bigg/\left(\frac{d\sigma}{d\Omega}\right)_{cl}$$

$$=\sum_{n'l'\in\bar{\omega},L}\frac{q^2}{2\omega}G^{HF,R}_{nl,n'l',L}(\bar{\omega},q). \tag{18}$$

If in experiments the excitation energy $\bar{\omega}$ is fixed with low accuracy, one can obtain the excitation cross section for the levels by integrating over q the expression (18), similarly to Eq. (17) and obtain

$$\sigma^{HF,R}_{nl}(\bar{\omega})=\sum_{n'l'\in\bar{\omega},L}\sigma^{HF,R}_{nl,n'l'}(\bar{\omega})$$

$$=2\pi\frac{c^2}{E^2}\int q\,dq\left(\frac{d\sigma}{d\Omega}\right)_{cl}\sum_{n'l'\in\bar{\omega},L}\xi^{HF,R}_{nl,n'l'}(\bar{\omega},q). \tag{19}$$

Using the known expression for the classical Thompson scattering cross section (see [2])

$$\left(\frac{d\sigma}{d\Omega}\right)_{cl}=\frac{1}{c^4}\left[1-\frac{1}{2}\left(\frac{qc}{E}\right)^2+\frac{1}{8}\left(\frac{qc}{E}\right)^4\right], \tag{20}$$

one obtains from Eq. (19)

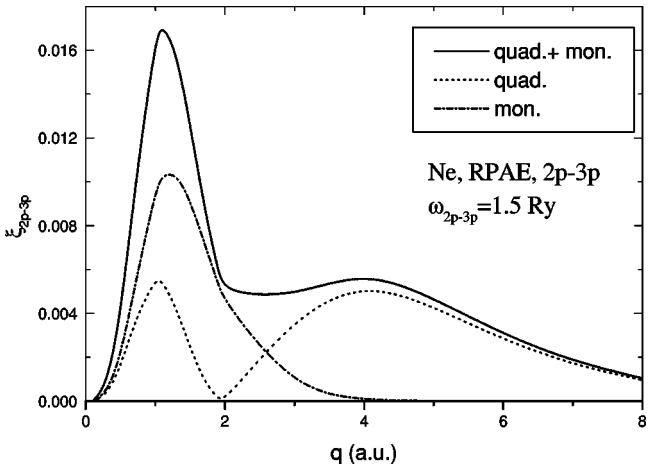

FIG. 1. Differential cross sections, relative to the Thompson differential cross section (DCS), in Compton scattering for monopole (dot-dashed curve) and quadrupole (dashed curve) excitations and their total (solid curve) for Ne $2p$-$3p$ transitions, calculated in RPAE at $\omega_{2p\text{-}3p}=1.5$ Ry.

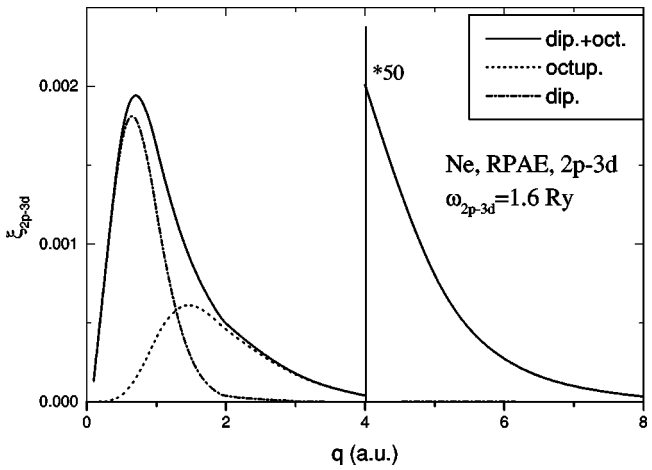

FIG. 2. Differential cross sections, relative to the Thompson DCS, in Compton scattering for dipole (dot-dashed curve) and octupole (dashed curve) excitations and their total (solid curve) for Ne $2p$-$3d$ transitions, calculated in RPAE at $\omega_{2p\text{-}3d}=1.6$ Ry.

$$\sigma_{nl}^{HF,R}(\overline{\omega})=\frac{2\pi}{E^2c^2}\int_0^{2E/c}qdq\left[1-\frac{1}{2}\left(\frac{qc}{E}\right)^2+\frac{1}{8}\left(\frac{qc}{E}\right)^4\right]\sum_{n'l'\in\overline{\omega},L}\xi_{nl,n'l'}^{HF,R}(\overline{\omega},q). \quad (21)$$

Since for a given set of discrete levels the sum in Eq. (21) decreases very fast with q growth, one can simplify Eq. (21) transforming it into the following expression:

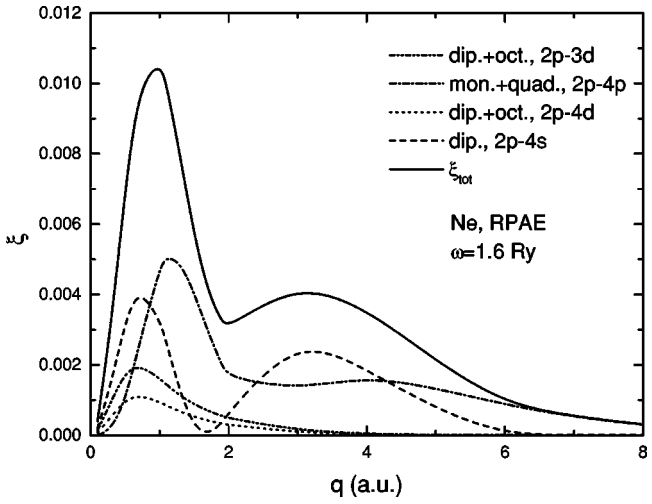

FIG. 3. Differential cross sections, relative to the Thompson DCS, in Compton scattering for monopole (dot-dashed curve) and quadrupole (dashed curve) excitations and their total (solid curve) for Ne $2p$-$4p$ transitions, calculated in RPAE at $\omega_{2p\text{-}4p}=1.6$ Ry. The total (solid curve) is the sum of the contributions of $2p$-$3d$, $2p$-$4p$, $2p$-$4s$, and $2p$-$4d$ excitations. Clearly seen in the figure is the fact that the $2p$-$4p$ transition dominates the sum.

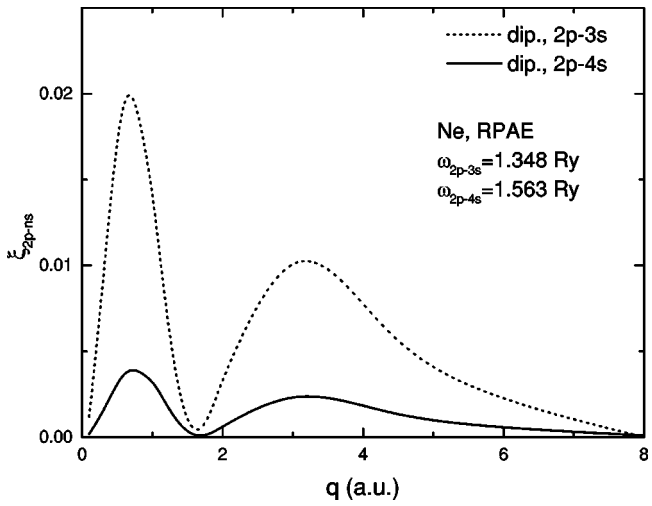

FIG. 4. Differential cross sections, relative to the Thompson DCS, in Compton scattering for dipole $2p$-$3s$ (dashed curve) and dipole $2p$-$4s$ (solid curve) excitations for Ne.

$$\sigma_{nl}^{HF,R}(\overline{\omega})\simeq\frac{3c^2}{4E^2}\sigma_{cl}\int_0^{q_{\max}}qdq\sum_{n'l'\in\overline{\omega},L}\xi_{nl,n'l'}^{HF,R}(\overline{\omega},q)\equiv\frac{3c^2}{4E^2}\sigma_{cl}A_{\overline{\omega},L,nl}^{HF,R}, \quad (22)$$

where $q_{\max}$ is the upper value of q: for $q>q_{\max}$ $\xi_{nl,n'l'}^{HF,R}(\overline{\omega},q)$ for a given set of discrete levels $n'l'\in\overline{\omega},L$ vanish. It is implied that $q_{\max}\ll 2E/c$.

The formula (22) will be used below to obtain the total discrete-level excitation cross section in the Compton scattering and to compare it to the total classical Thompson cross section of light scattering upon an electron $\sigma_{cl}=8\pi/3c^4\approx 2.3755\times10^{-8}$ a.u. For the cross section 1 a.u.$\approx$2.8002 $\times10^{-17}$ cm^2.

Let us note that the contribution of a group of discrete levels decreases with the growth of E as E^{-2}, while the total Compton cross section is almost E independent. This means

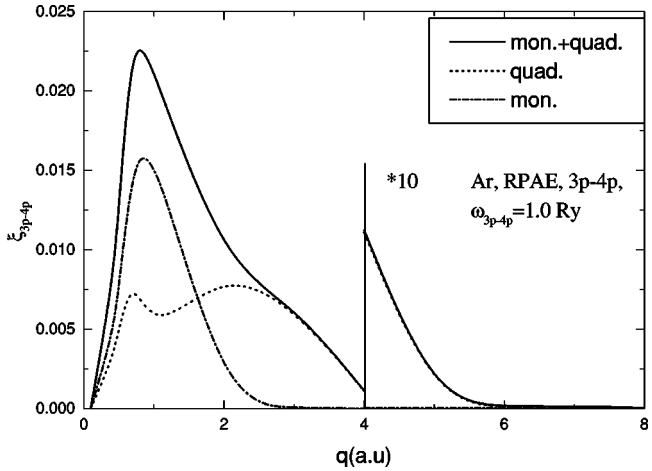

FIG. 5. Same as in Fig. 1, except that the results are for Ar $3p$-$4p$ transitions and $\omega_{3p\text{-}4p}=1.0$ Ry.

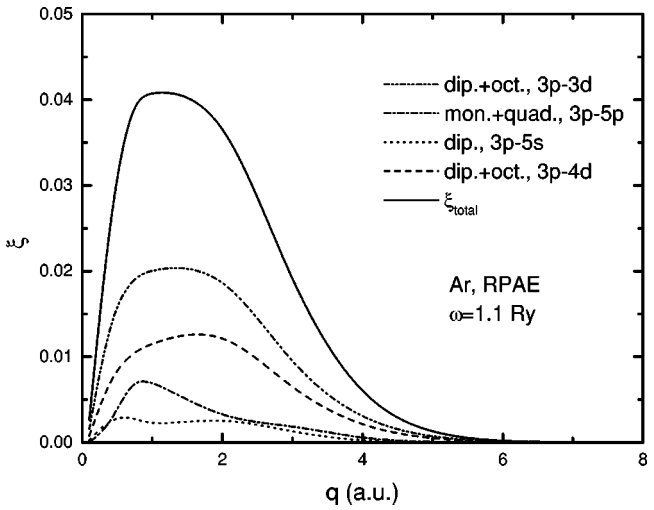

FIG. 6. Differential cross sections, relative to the Thompson DCS, in Compton scattering for dipole (dot-dashed curve) and octupole (dashed curve) excitations for Ar $3p$-$3d$ transitions, calculated in RPAE at $\omega_{3p\text{-}3d}=1.06$ Ry. The total (solid curve) is the sum of the contributions of $3p$-$3d$, $3p$-$5p$, $3p$-$5s$, and $3p$-$4d$ excitations, which is dominated by the $3p$-$3d$ transitions.

that with an increase of E the main contribution to the Compton cross section comes not from electron excitation but from atomic electrons ionization.

V. RESULTS

Our calculations were performed for the outer subshells discrete transitions $np-(n+1),(n+2)p$, $L=0,2$, $np-n,(n+1)d$ [$2p$-$3d$,$4d$ for Ne], $L=1,3$ and $np-(n+1),(n+2)s$, $L=1$ in Ne, Ar, Kr and Xe for the momentum transferred $q\leqslant 8$ a.u. The results are presented in Figs. 1–11, corresponding to Ne (Figs. 1–4), Ar (Figs. 5–7), Kr (Figs. 8 and 9) and Xe (Figs. 10 and 11).

The energy difference between the monopole and quadrupole levels considered is small for all the atoms investigated, just as the difference between the dipole and octupole levels. All energies presented below are in rydbergs. For Ne one has $\omega_{2p3p}^{L=0}=1.5023$, $\omega_{2p3p}^{L=2}=1.4739$, $\omega_{2p4p}^{L=0}=1.6074$, $\omega_{2p5p}^{L=2}=1.5981$, $\omega_{2p3d}^{L=1}=1.5886$, $\omega_{2p3d}^{L=3}=1.5888$, $\omega_{2p4d}=1.6379$, $\omega_{2p4d}^{L=3}=1.6379$, $\omega_{2p3s}=1.3481$, and $\omega_{2p4s}=1.5635$. This is why Fig. 1 presents the total values of $\xi_{2p,3p}^{R}(\omega,q)$ and its monopole and quadrupole components in RPAE for both $2p$-$3p$ transitions at the same energy $\omega_{2p3p}=1.5$. Figure 2 depicts the much smaller contribution of the dipole and octupole $2p$-$3d$ transitions to $\xi_{2p,3d}^{R}(\omega,q)$. The energy $\omega_{2p3d}\cong 1.589\simeq 1.6$ almost coincides with $\omega_{2p4p}=1.60\simeq 1.6$ and is close to $\omega_{2p4d}\simeq 1.64$, on the one hand, and $\omega_{2p4s}\simeq 1.564$ on the other, which makes them difficult to distinguish. This is why Fig. 3 presents the sum along with the partial contributions of the transitions $2p$-$3d$, $2p$-$4p$, $2p$-$4s$, and $2p$-$4d$. We see that for all q the contribution of the $2p$-$4p$ transition dominates, however the contribution of the $2p$-$4s$ transition

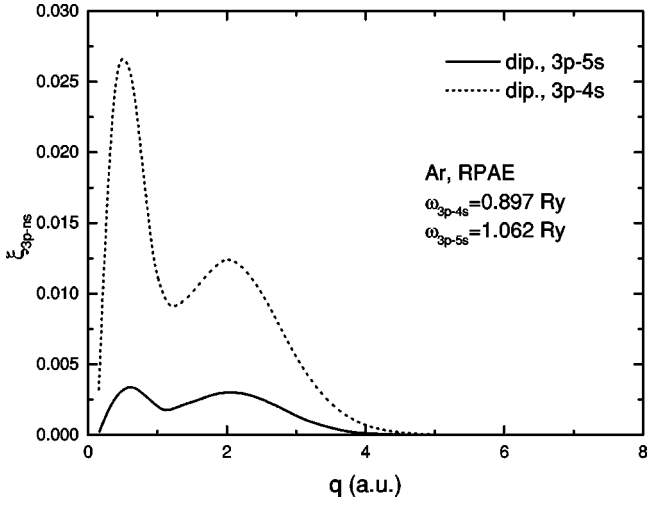

FIG. 7. Same as in Fig. 4, except that the results are for Ar $3p$-$4s$ (dashed curve) and $3p$-$5s$ (solid curve) and $\omega_{3p\text{-}5s}=1.062\,65$ Ry.

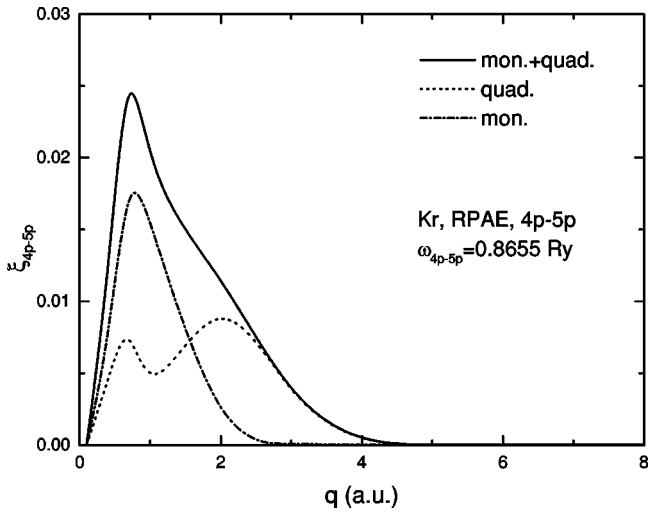

FIG. 8. Same as in Fig. 1, except that the results are for Kr $4p$-$5p$ transitions and $\omega_{4p\text{-}5p}=0.86$ Ry.

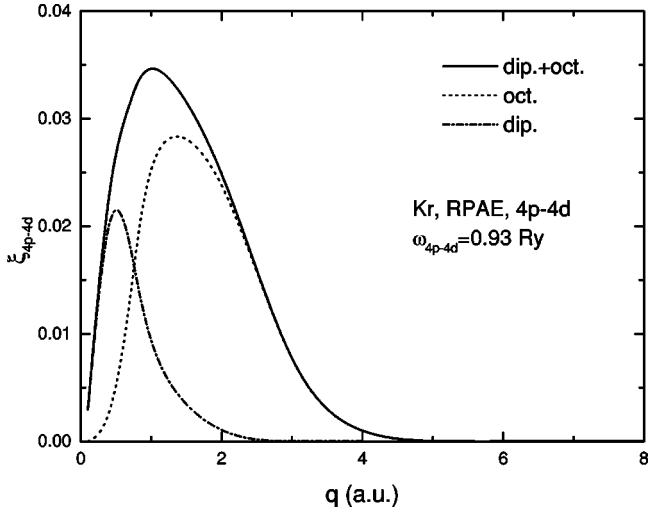

FIG. 9. Same as in Fig. 2, except that the results are for Kr $4p$-$4d$ transitions and $\omega_{4p\text{-}4d}=0.93$ Ry.

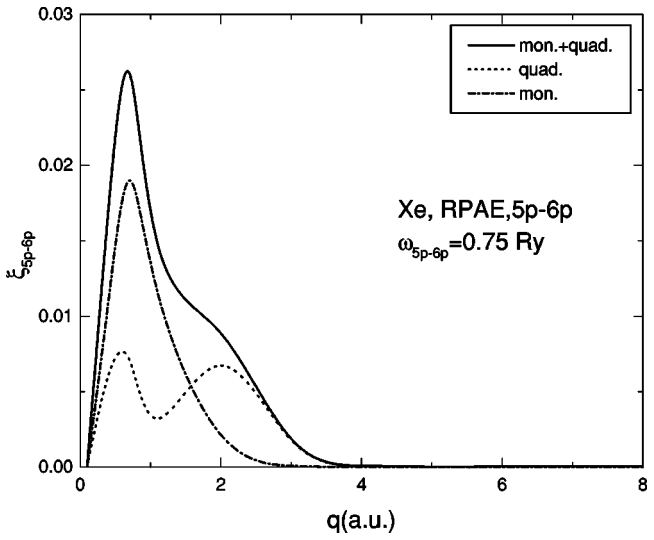

FIG. 10. Same as in Fig. 1, except that the results are for Xe $5p$-$6p$ transitions and $\omega_{5p\text{-}6p}=0.75$ Ry.

is almost as large. Figure 4 presents $\xi^R_{2p,3s}(\omega_{2p3s},q)$, which has a two-hump structure and is even larger than $\xi^R_{2p,3p}(\bar{\omega},q)$ at almost all q. Note that $\xi^R_{2p,3s}(\omega_{2p3s},q)$ is a factor of about 5 greater than $\xi^R_{2p,4s}(\omega_{2p4s},q)$.

Figure 5 presents $\xi^R_{3p,4p}(\bar{\omega},q)$ for the Ar $3p$-$4p$ monopole and quadrupole transitions and their sum. Again, the excitation energies here $\omega^{L=0}_{3p4p}=1.0068$ and $\omega^{L=2}_{3p4p}=1.0590$ are very close, so that the common energy is chosen to be equal to $\omega_{3p4p}=1.0$ Ry. Figure 6 presents the sum along with the partial contributions of all the transitions $3p$-$3d$, $3p$-$5p$, $3p$-$5s$, and $3p$-$4d$, which are close in energy. By far the dominant contribution comes from the $3p$-$3d$ transition, which is a direct consequence of the fact that this transition proceeds between states with the same principal quantum

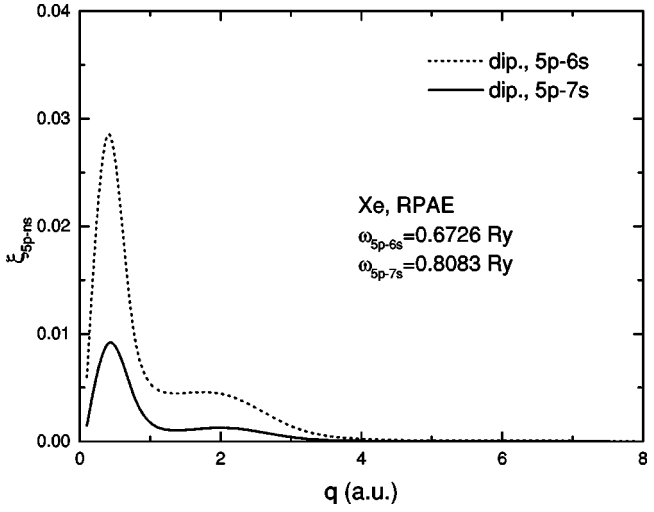

FIG. 11. Same as Fig. 4, except that the results are for Xe $5p$-$6s$ and $5p$-$7s$ dipole transitions with $\omega_{5p\text{-}6s}=0.672\,58$ Ry and $\omega_{5p\text{-}7s}=0.808\,28$ Ry.

number. Figure 7 presents the results for $\xi^R_{3p,4s}(\omega_{3p4s},q)$, which again, as in Ne, have a clear two-hump structure and are even larger than $\xi^R_{3p,4p}(\bar{\omega},q)$ at almost all q. Note that $\xi^R_{3p,4s}(\omega_{3p4s},q)/\xi^R_{3p,5s}(\omega_{3p5s},q)$ in Ar is greater than the ratio in Ne, but $\xi^R_{3p,4d}(\bar{\omega},q)$ is only a factor of about 2 smaller than $\xi^R_{3p,3d}(\bar{\omega},q)$.

Figure 8 depicts the total value of $\xi^R_{4p,5p}(\bar{\omega},q)$ and its monopole and quadrupole contributions in Kr. Contrary to the previous cases it is a factor of about 3 smaller than $\xi^R_{4p,4d}(\bar{\omega},q)$, presented in Fig. 9. We infer that dipole excitations can be quite probable in Compton scattering.

Figure 10 presents $\xi^R_{5p,6p}(\bar{\omega},q)$ for Xe and Fig. 11 presents $\xi^R_{5p,6s}(\omega,q)$ and $\xi^R_{5p,7s}(\bar{\omega},q)$ for Xe. Again the contribution of the dipole transition is larger. Clearly, the main features in all the Xe transitions considered are qualitatively similar to those for the other noble-gas atoms.

All the curves for $np-(n+1),(n+2)p$ excitations have a common qualitative feature. Namely, each curve has a strong maximum, which is pronounced mostly at $q\approx 1$. In all the curves an additional interesting peculiarity appears due to the quadrupole contribution, viz. they have two maxima, one at $q\approx 1$ and the second one, which moves from $q\approx 4$ in Ne to $q\approx 2$, in Xe. All curves for $np-(n+1),(n+2)s$ have a two-hump structure and the contribution of $np-(n+1)s$ is much larger than that of the $np-(n+2)s$. However, the curves for the p-d transitions, both dipole and octupole, at least in the q region considered, have a single maximum located for the dipole transition at lower q than that for the quadrupole. The strength of the latter increases rapidly as we move from Ne to Xe.

The values of total cross sections $\sigma^R_{nl}(\bar{\omega})$ according to Eq. (22) are characterized by the factors $A^R_{\bar{\omega},L,nl}$, which are $A^R_{\bar{\omega},L,2p}\simeq 0.2947$ for Ne, $A^R_{\bar{\omega},L,3p}\simeq 0.1939$ for Ar, $A^R_{\bar{\omega},L,4p}\simeq 0.2779$ for Kr, and $A^R_{\bar{\omega},L,5p}\simeq 0.3217$ for Xe. For energies that are of interest for Compton scattering, namely, for E bigger than tens of keV $c/E\ll 1$, $A^{HF,R}_{\bar{\omega},L,nl}<Z$ and therefore the discrete-level excitation cross section is much smaller than the total atomic classical Thompson scattering cross section $\sigma^{tot}_{cl}=8\pi Z/3c^4$.

VI. CONCLUSION

In this paper we have investigated both differential cross sections in angle and total cross sections for monopole, dipole, quadrupole, and octupole excitation of discrete atomic levels of Ne, Ar, Kr and Xe in Compton scattering. Results have been obtained in the HF approximation and with many-electron effects taken into account in the RPAE. However, to minimize the number of figures, only RPAE results have been presented, focusing on the relative importance of monopole, dipole, quadrupole, and octupole excitations.

Generally, we have found that the curves for the monopole, dipole, quadrupole and octupole excitations for the noble-gas atoms are characterized by maxima and minima as a function of q. A dominant peak occurs near $q=0$ in the

monopole excitation curves, while the characteristic peak for the quadrupole excitation appears at a larger q value. In contrast, the dipole peak occurs closer to $q=0$ in comparison with the characteristic peak for octupole excitation.

We conclude by noting that the main contribution to the Compton cross section at high energies comes from atomic electrons ionization and not their excitation.

ACKNOWLEDGMENTS

This research was supported by U.S. DOE, Division of Chemical Sciences, Office of Basic Energy Research, NSF, International Science and Technology Center, Project No. 1358 (M.Y.A. and L.V.C.) and the S. A. Shonbrunn Research Endowment Fund (M.Y.A.).

[1] J. A. R. Samson, C. H. Greene, and R. J. Bartlett, Phys. Rev. Lett. **71**, 201 (1993).
[2] V. B. Berestetskii, E. M. Lifshits, and L. P. Pitaevskii, *Relativistic Quantum Theory* (Oxford, Pergamon, 1974).
[3] J. C. Levin, G. B. Armen, and I. A. Selin, Phys. Rev. Lett. **76**, 1220 (1996).
[4] J. Ullrich, R. Moshammer, and R. Dorner *et al.*, J. Phys. B **30**, 2917 (1997).
[5] L. Young, R. W. Dunford, E. P. Kanter, B. Krassig, S. H. Southworth, R. A. Bonham, P. Lykos, C. Morong, A. Timm, J. P. J. Carney, and R. H. Pratt, Phys. Rev. A **63**, 052718 (2001).
[6] J. P. J. Carney and R. H. Pratt, Phys. Rev. A **62**, 012705 (2000).
[7] T. Suric, K. Pisk, B. A. Logan, and R. H. Pratt, Phys. Rev. Lett. **73**, 790 (1994).
[8] M. Ya. Amusia and A. I. Mikhailov, Phys. Lett. A **199**, 209 (1995).
[9] M. Ya. Amusia and A. I. Mikhailov, J. Phys. B **28**, 1723 (1995).
[10] T. Suric, K. Pisk, and R. H. Pratt, Phys. Lett. A **211**, 290 (1996).
[11] M. Ya. Amusia and A. I. Mikhailov, Sov. Phys. JETP **84**, 474 (1997).
[12] L. R. Andersson and J. Burgdörfer, Phys. Rev. Lett. **71**, 50 (1993).
[13] J. H. McGuire, *Electron Correlation Dynamics in Atomic Collisions* (Cambridge University Press, Cambridge, 1997).
[14] M. Ya. Amusia, *Atomic Photoeffect* (Plenum Press, New York, 1990).
[15] M. Ya. Amusia, A. S. Baltenkov, L. V. Chernysheva, Z. Felfli, and A. Z. Msezane, Phys. Rev. A **63**, 052506 (2001).
[16] M. Ya. Amusia, L. V. Chernysheva, Z. Felfli, and A. Z. Msezane, Surf. Rev. Lett. (to be published).
[17] H. A. Bethe, Ann. Phys. (Leipzig) **5**, 325 (1930); L. D. Landau and E. M. Lifshitz, *Quantum Mechanics, Non-relativistic Theory* (Pergamon, Oxford, 1974).
[18] M. Ya. Amusia, N. A. Cherepkov, L. V. Chernysheva, and S. T. Manson, Phys. Rev. A **61**, 020701(R) (2000).
[19] M. Ya. Amusia, A. S. Baltenkov, Z. Felfli, and A. Z. Msezane, Phys. Rev. A **59**, R2544 (1999).
[20] X. W. Fan and K. T. Leung, Phys. Rev. A **62**, 062703 (2000).
[21] A. Z. Msezane, Z. Felfli, M. Ya. Amusia, Z. Chen, and L. V. Chernysheva, Phys. Rev. A **65**, 054701 (2002).
[22] M. Ya. Amusia and L. V. Chernysheva, *Computation of Atomic Processes* (IOP Publishing, Bristol, 1997).